Theoret. Chim. Acta (Berl.) 64, 293–311 (1984)

THEORETICA CHIMICA ACTA

# A molecular orbital study of the rotation about the C–C bond in 1,3-butadiene

**Charles W. Bock**

Chemistry Department, Philadelphia College of Textiles & Science, Philadelphia,
Pennsylvania 19144, USA

**Philip George**

Biology Department, University of Pennsylvania, Philadelphia, Pennsylvania 19104, USA

**Mendel Trachtman**

Chemistry Department, Philadelphia College of Textiles & Science, Philadelphia,
Pennsylvania 19144, USA

The geometry and energy of 1,3-butadiene have been calculated using the 6-311G** basis set as a function of the CCCC dihedral angle–0° (*trans*), 30°, 60°, 75°, 90°, 120°, 135°, 150°, 165° and 180° (*cis*)–assuming that the vinyl groups remain planar. Potential minima are located at 0° and 141.4°, with the *trans* structure more stable than the *gauche* by 13.2 kJ mol$^{-1}$. Potential maxima are located at 76.7°, giving a barrier height of 25.4 kJ mol$^{-1}$ relative to the *trans* structure, and at 180° giving a barrier height of 3.0 kJ mol$^{-1}$ relative to the 141.4°-*gauche* structure. Using the 6-31G* basis set the inclusion of electron correlation, accounting for about 52% of the correlation energy, was found to produce no significant change in the shape of the potential energy curve. The magnitude of the expectation energy differences is such that both barriers with respect to the 141.4°-*gauche* maximum structure can be categorized unequivocally as attractive-dominant, whereas the values for the energy barrier with respect to the *trans* structure, although characteristic of a repulsive-dominant barrier at the 6-311G** level, are sufficiently small that higher level calculations might give the opposite result. Analysis of $\Delta V_{nn}$ for the conversion reactions *cis* → 150°-*gauche*, *trans* → 60°-*gauche*, and *trans* → 90°-*gauche* in terms of the individual contributions from the various

---

Offprint requests to: P. George

internuclear interactions shows that nonbonded interactions are important, not only in initiating the destabilization of the crowded *cis* structure, but also through-out the entire range of CCCC dihedral angles, 0° to 180°.

**Key words:** 1,3-butadiene—Rotational barrier.

## 1. Introduction

It is well-established by electron diffraction, far infrared, infrared, NMR, microwave and Raman studies that the most stable conformer of 1,3-butadiene is the planar *trans* structure, see the references listed by Carreira [1]. But there are conflicting reports concerning the nature of the second less stable conformer, some favoring the planar *cis* structure [1–3], and others a nearby *gauche* structure resulting from a small rotation about the central C—C bond [4–6]. Furthermore it has been suggested that the energy difference between such a *gauche* structure and the *cis* structure might be so small that the zero-point torsional level would probably lie above the potential energy for the *cis* structure, making any distinction almost meaningless [2, 3]. In addition, to calculate the torsional potential energy curve from experimental data assumptions and/or approximations had to be made [7]. In view of these uncertainties, the results of molecular orbital calculations take on added significance.

Without exception the calculations reported in the literature, no matter whether utilizing standard geometry with rigid or flexible rotation [8], a rigid rotation model and an experimental *trans* geometry [8–12], or geometry optimization [12], all agree in predicting the trans conformer to be the most stable in accord with experiment. With only one exception [9], the second less stable conformer is predicted to be a *gauche* and not the *cis* structure, see Table 1. It is to be noted, however, that in the majority of the calculations the energy difference $[E_T(cis) - E_T(gauche)]$ is quite small, about 3 kJ $mol^{-1}$ or less, and in one set of calculations in particular [8] the potential energy curve was found to be very flat in the region 150° to 180° (*cis*).

The height of the energy barrier separating the *trans* conformer and the less stable *cis* (or *gauche*) conformer calculated from spectroscopic data ranges from 24 to 32 kJ $mol^{-1}$ [7], compared to a value of 21 kJ $mol^{-1}$ derived from calorimetric data [18], and a value of about 30 kJ $mol^{-1}$ obtained by combining $\Delta H_0^\circ$ for the *trans* → *cis* conversion, 3.2 kcal $mol^{-1}$, as determined by Mui and Greenwald [3], and an estimate of $\Delta H^{\neq}$ for the *cis* → *trans* conversion, 3.9 kcal-$mol^{-1}$, reported by Squillacote et al. [2]. The values calculated *ab initio* all lie well within the range of these experimental values, see Table 1.

The previous calculations utilizing geometry optimization [12] did not explore the extent to which the potential energy curve is affected by the inclusion of polarization functions and electron correlation. Although CI was included in two of the other studies reported in the literature the results are in disagreement, a *gauche* structure being favored with respect to the *cis* in one case [9] and

**Table 1.** The nature of the second stable conformer of 1,3-butadiene, and the *gauche* barrier with respect to rotation about the C—C bond, according to various *ab initio* calculations

| Reference | Geometry | Rotation | Basis set | Second stable conformer$^{a}$ | $E_T$(cis)– $E_T$(*gauche*) kJ mol$^{-1}$ | $E_T$(*trans*) a.u. | Barrier ∠CCCC$^{a}$ | $E_T$(barrier)– $E_T$(*trans*) kJ mol$^{-1}$ |
|---|---|---|---|---|---|---|---|---|
| 8 | standard | rigid | STO-3G | 140°-*gauche* | +10 | — | 85° | 28.1 |
| 8 | standard | flexible$^{b}$ | STO-3G | *gauche*≈*cis*$^{c}$ | ≈0 | −153.01661 | 85° | 28.2 |
| 8 | exptl. *trans* [13] | rigid | STO-3G | *gauche*≈*cis*$^{c}$ | ≈0 | — | 85° | 27.7 |
| 9 | exptl. *trans* [14] | rigid | (10,5/5) | *cis* | −2.1$^{d}$ | −154.8214 | ~90°$^{e}$ | 31.8 |
| 9 | exptl. *trans* [14] | rigid | (10,5/5)+CI$^{f}$ | 135°-*gauche* | +0.8 | −154.8579 | ~90°$^{e}$ | 26.5 |
| 10 | exptl. *trans* [15, 16] | rigid | (7,3/3) | 145°-*gauche* | +3.3 | −154.4643 | 80° | 29.9 |
| 10 | exptl. *trans* [15, 16] | rigid | (7,3/3)+CI$^{g}$ | 157°-*gauche* | +0.4 | −154.7309 | 80° | 27.7 |
| 11 | exptl. *trans* [17] | rigid | (7,3/4) | 140°-*gauche* | +7.5 | −154.69313 | 80° | 28.0 |
| 11 | exptl. *trans* [17] | flexible$^{h}$ | (7,3/4) | 140°-*gauche* | +1.7 | −154.69313 | 80° | 27.6 |
| 11 | exptl. *trans* [17] | flexible$^{i}$ | (9,5/4) | 140°-*gauche* | +2.1 | −154.83630 | 80° | 25.1 |
| 12 | exptl. *trans* [15] | rigid | (7,3/4) | 140°-*gauche* | +6.9 | −154.74285 | ~90°$^{e}$ | 25.9 |
| 12 | optimized$^{j}$ | flexible$^{j}$ | (7,3/4) | 140°-*gauche* | +2.5 | −154.74609 | ~90°$^{e}$ | 23.8 |

[a] Taking the CCCC dihedral angle in the *trans* structure as zero

[b] Optimization of the CCC valence angle

[c] The potential energy curve is very flat in the region ∠CCCC = 150° to 180°

[d] With respect to the 135°-*gauche* structure

[e] ∠CCCC for the barrier not located any more precisely

[f] Accounting for about 4% of the correlation energy, see Appendix

[g] Accounting for about 26% of the correlation energy, see Appendix

[h] Optimization of the CCC valence angle and the C—C bond length

[i] CCC valence angles and C—C bond lengths as in (*h*)

[j] Assuming that the vinyl groups remain planar, but otherwise with full geometry optimization

vice-versa in the other [10], see Table 1. This could be a consequence of the use of *trans* geometries that were not optimized at the SCF level, the rigid rotation model employed, and the very different extent to which the correlation energy is accounted for.

The calculations reported in this paper have been carried out to explore these two aspects. As Skaarup et al. did [12], it has been assumed that the vinyl groups remain planar throughout the rotation about the C—C bond, but otherwise full geometry optimization has been employed.

The changes in bond lengths and bond angles, and the resulting change in nuclear repulsion energy indicative of a relaxation or contraction of the structure, are correlated with the change in total molecular energy as the CCCC dihedral angle is varied from 0° (*trans* structure) to 180° (*cis* structure). To analyse the relaxation or contraction of the structure in greater detail, a distinction has been made between internuclear distances, which, in a rigid rotation model, would be dependent upon the dihedral angle, and those which would not. In this way it becomes possible to assess the relative importance of changes in the geometry of the nuclear framework as distinct from changes due solely to the rotation of its component parts.

## 2. Computational details

All the calculations were carried out on a VAX 11/780 computer including a floating point accelerator using a modified version [19] of the Gaussian 80 program [20]. The standard basis sets 6-31G [21], 6-31G* [22] and 6-311G** [23] with gradient optimization were employed. To explore the effect of electron correlation further calculations were carried out with the HF/6-31G* optimized geometry using Møller–Plesset perturbation theory to second order (MP2) and to third order (MP3), and, in addition, configuration interaction (CI) using all double substitutions from the reference HF/6-31G* determinant. In the latter case the size correction introduced by Pople et al. [24] was also incorporated.

As an indication of the magnitude of these calculations typical CPU times for one of the nonplanar structures were: 6-31G* geometry optimization about 6 h, 6-311G** geometry optimization about 35 h, and a CID calculation using the 6-31G* optimized geometry about 60 h.

## 3. Results

### 3.1. Energy

The values of $E_T$ for 1,3-butadiene at various CCCC dihedral angles, calculated using the 6-311G** basis set are listed in Table 2. The plot of these data in Fig. 1 shows potential minima at 0°, the *trans* structure, and at 141.4° for a *gauche* structure, with the latter less stable by 13.2 kJ $\text{mol}^{-1}$. The potential maxima are at 76.7°, giving a barrier height of 25.4 kJ $\text{mol}^{-1}$ relative to the *trans* structure, and at 180°, the *cis* structure, giving a barrier height of 3.0 kJ $\text{mol}^{-1}$ relative to

**Table 2.** Total molecular energy, $E_T$, and the nuclear repulsion energy, $V_{nn}$, for 1,3-butadiene as a function of the CCCC dihedral angle, calculated using the 6-311G** basis set

| Dihedral angle | $E_T$ a.u. (+154) | $V_{nn}$ a.u. (−100) |
|---|---|---|
| 0° (*trans*) | −0.96054 | +4.35036 |
| 30° | −0.95732 | +4.28738 |
| 60° | −0.95146 | +4.26625 |
| 75° | −0.95087 | +4.37111 |
| 90° | −0.95126 | +4.56067 |
| 120° | −0.95440 | +5.10782 |
| 135° | −0.95540 | +5.29528 |
| 150° | −0.95533 | +5.32838 |
| 165° | −0.95470 | +5.26320 |
| 180° (*cis*) | −0.95437 | +5.22662 |

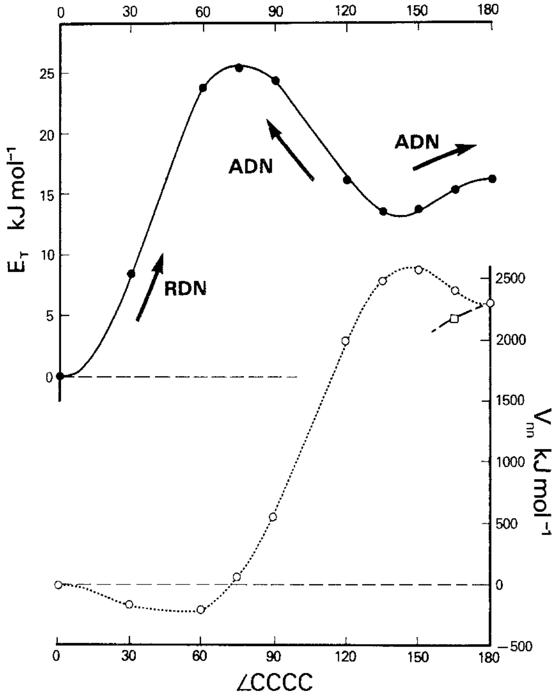

**Fig. 1.** Plots of the total molecular energy, $E_T$, and the nuclear repulsion energy, $V_{nn}$, for 1,3-butadiene relative to the values for the *trans* structure, as a function of the CCCC dihedral angle. The maximum and minimum in the $E_T$ curve at 76.7° and 141.4° respectively, and in the $V_{nn}$ curve at 145.9 and 61.1° respectively, have been calculated from the nearest three sets of data points in each case

the 141.4°-*gauche* structure. These will be referred to as the *gauche* and the *cis* barrier respectively.

Similar calculations using the 6-31G* basis set give $E_T$ values about 0.0415 a.u. less negative, however the shape of the potential energy curve remains unaltered as shown by the $E_T$ increments in Table 3, which at most differ by 0.1 kJ mol$^{-1}$. The inclusion of electron correlation at this level, which results in $E_T$ values up to 0.54 a.u. more negative, leads to only minor changes in the shape of the curve. Taking the values for E(CI, size corrected), which gives the maximum improve-

**Table 3.** Total molecular energies for 1,3-butadiene at various CCCC dihedral angles calculated using the 6-311G** basis set, the 6-31G* basis set, and the latter including electron correlation, together with the energy increments which serve to characterize the shape of the potential energy curve

| | CCCC dihedral angle | | | | |
|---|---|---|---|---|---|
| Basis set | 0° *trans* | 90° | 120° | 150° | 180° *cis* |
| HF/6-311G** | −154.96054 | −154.95126 | −154.95440 | −154.95533 | −154.95437 |
| HF/6-31G* | −154.91905 | −154.90973 | −154.91288 | −154.91384 | −154.91284 |
| MP2/6-31G* | −155.41534 | −155.40630 | −155.40955 | −155.41071 | −155.40964 |
| MP3/6-31G* | −155.44993 | −155.44145 | −155.44442 | −155.44542 | −155.44439 |
| CI/6-31G* | −155.38211 | −155.37346 | −155.37649 | −155.37743 | −155.37637 |
| CI, size corr./6-31G* | −155.45634 | −155.44808 | −155.45095 | −155.45191 | −155.45091 |

| Basis set | $E_T(150°)-E_T(0°)$ kJ mol$^{-1}$ | $E_T(90°)-E_T(0°)$ kJ mol$^{-1}$ | $E_T(120°)-E_T(150°)$ kJ mol$^{-1}$ | $E_T(180°)-E_T(150°)$ kJ mol$^{-1}$ |
|---|---|---|---|---|
| HF/6-311G** | 13.7 | 24.4 | 2.4 | 2.5 |
| HF/6-31G* | 13.7 | 24.5 | 2.5 | 2.6 |
| MP2/6-31G* | 12.2 | 23.7 | 3.0 | 2.8 |
| MP3/6-31G* | 11.8 | 22.3 | 2.6 | 2.7 |
| CI/6-31G* | 12.3 | 22.7 | 2.5 | 2.8 |
| CI, size corr./6-31G* | 11.6 | 21.7 | 2.5 | 2.6 |

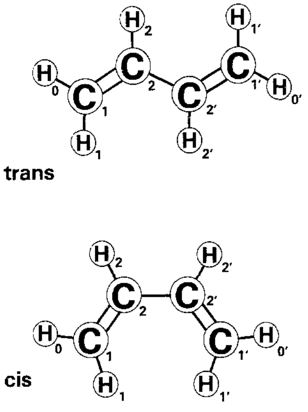

**Fig. 2.** The structures of *trans* and *cis* 1,3-butadiene drawn according to the geometry calculated using the 6-311G** basis set, with the number scheme used to identify the bond lengths and angles

ment in $E_T$ and accounts for about 52% of the correlation energy[1], the 150°-structure (in the region of the *gauche* maximum) becomes 2.1 kJ mol$^{-1}$ more stable relative to the *trans* structure, and the 90°-structure (near the *gauche* barrier) becomes 2.7 kJ mol$^{-1}$ more stable relative to the *trans* structure. However the shape of the curve in the region of the *gauche* minimum is still unaltered, the $E_T$ increments changing by only 0.1 kJ mol$^{-1}$, see Table 3.

It is interesting to compare these results with those obtained by Skaarup et al. [12] using a (7, 3) basis set and similar geometry optimization which gives $E_T$ values about 0.214 a.u. less negative than those obtained using the 6-311G** basis set. Assuming a dihedral angle of 140° for the *gauche* minimum, the energy difference relative to the *trans* structure was found to be 12.0 kJ mol$^{-1}$, the height of the barrier at 90° to be 23.8 kJ mol$^{-1}$, and the energy difference between the *gauche* and *cis* structures to be 2.5 kJ mol$^{-1}$.

It would thus appear that the shape of the potential energy curve for rotation about the C—C bond in 1,3-butadiene is very little affected by the addition of either polarization functions or the inclusion of electron correlation to basis sets of about double-zeta quality.

### 3.2. Geometry

Bond lengths and angles for 1,3-butadiene at various CCCC dihedral angles, calculated using the 6-311G** basis set, are listed in Table 4. Comparing these values, rounded off to 0.001 Å and 0.1°, with those obtained by Skaarup et al. [12] given in parentheses in the table shows that the use of the more extended basis set with the inclusion of polarization functions makes relatively little difference to the C=C bond length, increasing it by only 0.001–0.002 Å. The C—C bond length, on the other hand, is increased by 0.005–0.007 Å, and all three types of C—H bond are increased in length by 0.004–0.005 Å. The bond angles, however, are very little affected. In ten cases there is a slight decrease, by about 0.3° on average: in three cases a slight increase, less than 0.2° on average: and

---

[1] See Appendix for the calculation.

**Table 4.** Geometry of 1,3-butadiene as a function of the CCCC dihedral angle, calculated using the 6-311G** basis set, assuming that the vinyl groups remain planar but otherwise with full geometry optimization. The numbering scheme used to identify the bond lengths and angles is given in Fig. 2

| Parameter | 0° *trans*[a] | 30° | 60° | 75° | 90°[a] | 120° | 135°[b] | 150° | 165° | 180° cis[a] |
|---|---|---|---|---|---|---|---|---|---|---|
| $C_1{=}C_2$ | $1.321_8$ (1.320) | $1.320_6$ | $1.318_5$ | $1.317_8$ | $1.317_8$ (1.316) | $1.319_3$ | $1.320_0$ (1.319) | $1.320_8$ | $1.321_1$ | $1.321_4$ (1.320) |
| $C_2{-}C_{2'}$ | $1.467_4$ (1.463) | $1.475_1$ | $1.488_0$ | $1.490_5$ | $1.489_6$ (1.484) | $1.481_8$ | $1.479_2$ (1.474) | $1.478_7$ | $1.480_0$ | $1.480_1$ (1.473) |
| $C_1{-}H_0$ | $1.075_2$ (1.071) | $1.075_3$ | $1.075_8$ | $1.075_9$ | $1.076_0$ (1.072) | $1.075_7$ | $1.075_5$ (1.071) | $1.075_1$ | $1.074_9$ | $1.074_8$ (1.071) |
| $C_1{-}H_1$ | $1.077_2$ (1.073) | $1.077_4$ | $1.077_5$ | $1.077_2$ | $1.076_9$ (1.072) | $1.076_5$ | $1.076_4$ (1.072) | $1.076_3$ | $1.076_1$ | $1.076_0$ (1.072) |
| $C_2{-}H_2$ | $1.078_6$ (1.074) | $1.078_6$ | $1.079_1$ | $1.079_6$ | $1.080_0$ (1.075) | $1.080_1$ | $1.079_4$ (1.074) | $1.078_8$ | $1.078_3$ | $1.078_1$ (1.074) |
| $\angle C_1C_2C_{2'}$ | $124.0_4$ (124.7) | $124.0_4$ | $124.1_6$ | $124.3_4$ | $124.5_2$ (124.4) | $124.8_2$ | $125.3_2$ (125.2) | $126.1_2$ | $126.9_0$ | $127.2_3$ (127.0) |
| $\angle H_0C_1C_2$ | $121.5_3$ (121.8) | $121.4_8$ | $121.3_1$ | $121.2_4$ | $121.2_3$ (121.6) | $121.2_9$ | $121.1_6$ (121.5) | $121.0_0$ | $120.8_2$ | $120.7_4$ (121.1) |
| $\angle H_1C_1C_2$ | $121.6_2$ (121.8) | $121.6_9$ | $121.7_5$ | $121.7_6$ | $121.7_0$ (121.8) | $121.5_8$ | $121.7_5$ (121.8) | $122.1_3$ | $122.5_5$ | $122.7_4$ (122.7) |
| $\angle H_2C_2C_1$ | $119.6_0$ (119.6) | $119.4_6$ | $119.2_3$ | $119.1_9$ | $119.2_3$ (119.4) | $119.2_1$ | $119.0_1$ (119.3) | $118.6_2$ | $118.1_7$ | $118.0_1$ (118.2) |
| $H_0 \cdots H_1$ | $1.833_7$ | $1.833_8$ | $1.835_4$ | $1.835_8$ | $1.836_4$ | $1.836_4$ | $1.835_7$ | $1.833_2$ | $1.830_3$ | $1.829_2$ |
| $C_1 \cdots C_{1'}$ | $3.672_2$ | $3.632_2$ | $3.519_3$ | $3.441_8$ | $3.355_2$ | $3.178_5$ | $3.116_4$ | $3.085_6$ | $3.078_8$ | $3.079_2$ |

[a] Values in parentheses from reference 12: (7,3) → (5,3) basis set with similar geometry optimization.

[b] Values in parentheses at 140° from Ref. [12].

in three cases there is no change. Comparison with experimental values for the *trans* conformer [15], an electron diffraction $r_\alpha^0$ structure, shows the 6-311G** basis set underestimates the C=C bond length by 0.020 Å, overestimates the C—C bond length by 0.004 Å, and underestimates the C—H bond lengths by about 0.016 Å.

With the greater number of points at dihedral angles between 0° and 180° it is now possible to establish the geometrical character of the structure corresponding to the *gauche* minimum and the *gauche* barrier more precisely. To do this, the bond lengths C=C, C—C, $C_1$—$H_0$, $C_1$—$H_1$ and $C_2$—$H_2$, the bond angle $C_1$=$C_2$—$C_{2'}$ and the non-bonded distances $H_0 \cdots H_{0'}$ and $C_1 \cdots C_{1'}$ are plotted as a function of the dihedral angle in Figs. 3, 4 and 5.

In addition to the gross features which show nonbonded repulsions to be present in the *cis* structure, namely the opening out the C=C—C angle by about 3° relative to that in the *trans* structure [8, 11], and the tilting outward of the methylene groups [12], the calculations at the 6-311G** level provide further evidence for diminished electron delocalization in the *cis* structure. Not only is the C—C bond longer than in the *trans* structure by about 0.01 Å [12] i.e. less double bond character, but the C=C bond is a little shorter, i.e. more double bond character. As well as the outward tilt of the methylene group in the *cis* structure, as shown by the decrease in $\angle H_0C_1C_2$ of 0.8° and the increase in

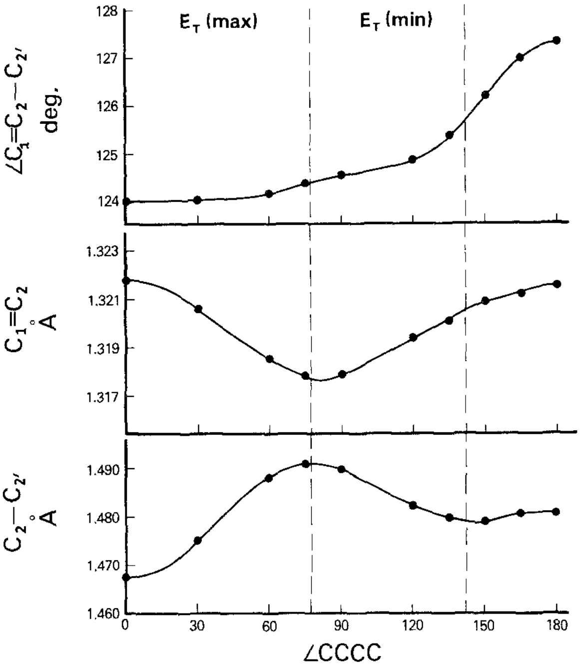

**Fig. 3.** The carbon–carbon bond lengths, $C_2$—$C_{2'}$ and $C_1$=$C_2$, and the bond angle $\angle C_1$=$C_2$—$C_{2'}$ as a function of the dihedral angle $\angle$CCCC

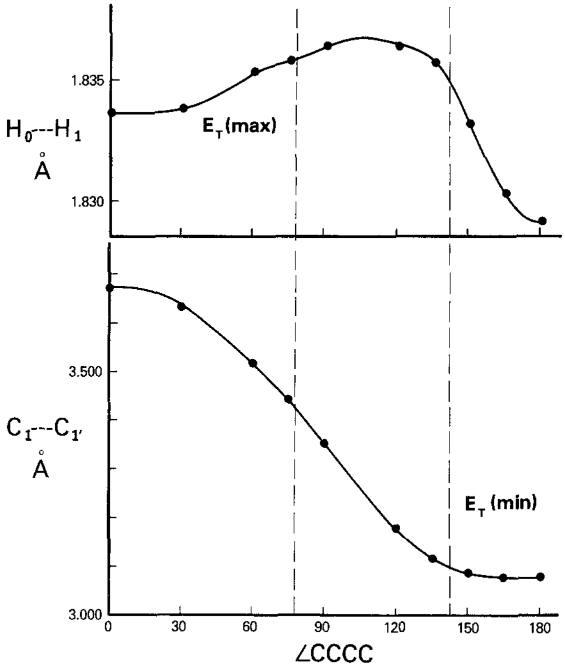

**Fig. 4.** The distance between the nonbonded atoms $H_0 \cdots H_1$ and $C_1 \cdots C_{1'}$ as a function of the dihedral angle ∠CCCC

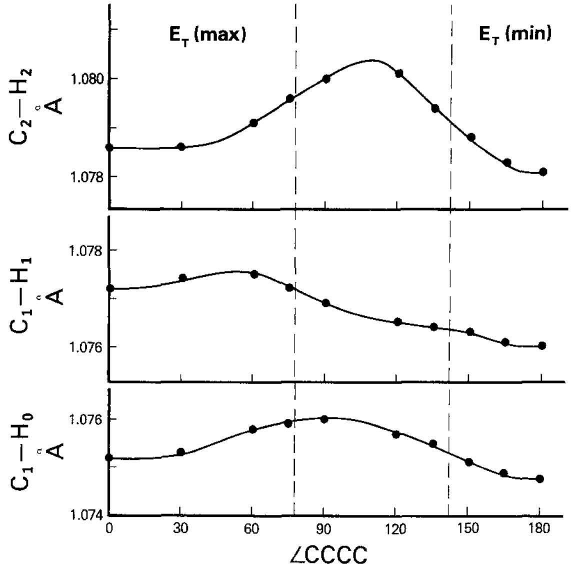

**Fig. 5.** The carbon–hydrogen bond lengths $C_1—H_0$, $C_1—H_1$ and $C_2—H_2$, as a function of the dihedral angle ∠CCCC

$\angle H_1C_1C_2$ of 1.1°, these changes also serve to bring the two hydrogen atoms closer together, i.e. $H_0 \cdots H_1$ decreases by 0.0045 Å, see Fig. 4.

In general terms one can consider the 141.4°-*gauche* structure to be more stable than the *cis* because nonbonded repulsions prevent the C=C bond length from reaching what otherwise would be a slightly larger maximum value, and the C—C bond length from what otherwise would be a considerably smaller minimum value as the CCCC dihedral angle approaches 180°.

The crucial difference between the *cis* and the slightly more stable 141.4°-*gauche* structure is revealed by the nuclear repulsion energy, which, as shown in Fig. 1, passes through a maximum over the same range of CCCC dihedral angles where the total molecular energy passes through a minimum. Relative to the *cis* structure the 141.4°-*gauche* structure is thus more compact, even though rigid rotation from the *cis* geometry would result in the structure opening out and $V_{nn}$ becoming less positive, see the dotted curve in Fig. 1. This more compact structure is attributable to the decrease in C=C and C—C bond lengths, and particularly to the decrease in the ∠C=C—C angle, see Fig. 3, so that there is no significant increase in the distance between the terminal carbon atoms as the dihedral angle changes from 180° to 150°, see Fig. 4.

In their study using a rigid rotation model and the (7, 3) basis set, Skancke and Boggs found the *gauche* barrier to occur at a dihedral angle a little more than 80° (see Fig. 2, reference 11). With geometry optimization and the 6-311G** basis set the angle is a little less, 76.7°, see Fig. 1. Although the C—C bond length reaches its maximum value at about this angle, the minimum C=C bond length is at a distinctly larger angle, about 83°, see Fig. 3. It may also be noted that the progressive decrease in $\angle C_1C_2C_{2'}$ in going from the stable *gauche* to the *trans* structure shows scarcely any perturbation in the region of 76.7°, see Fig. 3.

Although the variation of the C—H bond lengths with dihedral angle is considerably smaller than the variation for the C=C and C—C bonds there are nevertheless quite regular trends, see Fig. 5. However there is no correlation with the maximum and minimum in the potential energy curve at 76.7° and 141.4° respectively. The $C_1$—$H_0$ bond length has its maximum value at about 95°, the $C_1$—$H_1$ bond length at about 45°, and the $C_2$—$H_2$ bond length at about 105°. The ∠HCC bond angles also show regular trends, but there are no maxima (or minima). $\angle H_0C_1C_2$ and $\angle H_2C_2C_1$ stay fairly constant as the dihedral angle is increased from 0° to 120°, and then decrease a little from 120° to 180°: $\angle H_1C_1C_2$, on the other hand, stays fairly constant and then increases a little, see Table 3.

Finally, the plot of $V_{nn}$ in Fig. 1 reveals a feature of *gauche* structures in proximity to the *trans* which complements that of *gauche* structures in proximity to the *cis*. Rigid rotation at the *cis* geometry results in *gauche* structures with a less positive $V_{nn}$, but calculation with geometry optimization finds $V_{nn}$ more positive, i.e. these *gauche* structures are more compact relative to the *cis*, see above. Rigid rotation at the *trans* geometry, on the other hand, results in *gauche* structures with a more positive $V_{nn}$, but calculation with geometry optimization finds $\Delta V_{nn}$ less positive, i.e. these *gauche* structures are less compact relative to the *trans*. This feature persists over quite a wide range of dihedral angles, from 0° to about 74°, with a minimum $V_{nn}$ value of $-220.3\ \mathrm{kJ\,mol^{-1}}$ at 61.1°. It is to be noted that the *gauche* structure with a $V_{nn}$ of zero occurs at a dihedral angle, 74°, very close to that for the *gauche* barrier, 76.7°. However this may be fortuitous.

### 3.3. *The nature of the energy barriers* [25–27]

The finding that $V_{nn}$ is at a maximum at a CCCC dihedral angle very close to that for the *gauche* minimum, see Fig. 1, implies that $\Delta V_{nn}$ for the approach to either the *cis* barrier or the *gauche* barrier from the *gauche* minimum is negative. Now for chemical reactions and the more "mechanical" type of molecular process, e.g. rotation, it has been found [28] that $\Delta V_{nn} \approx \Delta V_{ee}$, and as a consequence, except in some rare cases for which $\Delta V_{nn}$, $\Delta V_{ee}$ and $\Delta V_{en}$ are very small and comparable in magnitude to $\Delta E_T$, $\Delta V_{nn}$ has the same sign as the total repulsion energy,

$$\Delta E_{\mathrm{rep}} = \Delta E_K + \Delta V_{ee} + \Delta V_{nn}.$$

Hence, with $\Delta V_{nn}$ negative, for $\Delta E_T$ to be positive the attraction energy term $\Delta V_{en}$ must be positive, and thus these two barriers with respect to rotation from the *gauche* minimum structure can be unequivocably classified as "attractive-dominant" [25–28]. Taking either the 135°-*gauche* or the 150°-*gauche* structure as typical of the *gauche* minimum, and the 75°-*gauche* structure as typical of the *gauche* barrier, the decomposition of $\Delta E_T$ in terms of $\Delta V_{nn}$ and $\Delta E_{\mathrm{elec}}$ is given in Table 5, (i) a and b, and (ii) a and b.

On the other hand the finding that the dihedral angle for the *gauche* barrier is so very close to the value at which $V_{nn}$ is the same as that for the *trans* structure,

**Table 5.** Expectation energy differences[a] characterizing the barriers to rotation about the C—C bond in 1,3-butadiene, calculated using the 6-311G** basis set

| | Approach to barrier | $\Delta V_{nn}$ | $\Delta E_{\mathrm{elec}}$ | $\Delta E_T$[b] | Type[c] |
|---|---|---|---|---|---|
| (i) a | 135°-*gauche* structure→ barrier (*cis* structure) | −0.06866 | +0.06969 | +0.00103 (2.7) | ADN |
| (i) b | 150°-*gauche* structure→ barrier (*cis* structure) | −0.10176 | +0.10272 | +0.00096 (2.5) | ADN |
| (ii) a | 135°-*gauche* structure→ barrier (75°-*gauche* structure) | −0.92417 | +0.92870 | +0.00453 (11.9) | ADN |
| (ii) b | 150°-*gauche* structure→ barrier (75°-*gauche* structure) | −0.95727 | +0.96173 | +0.00446 (11.7) | ADN |
| (iii) | *trans*-structure→ barrier (75°-*gauche* structure) | +0.02075 | −0.01108 | +0.00967 (25.4) | RDN |

[a] Values in a.u., except those in parentheses which are in $\mathrm{kJ\,mol^{-1}}$.

[b] $\Delta E_T = \Delta V_{nn} + \Delta E_{\mathrm{elec}}$, where $\Delta E_{\mathrm{elec}} = \Delta E_K + \Delta V_{ee} + \Delta V_{en}$.

[c] ADN and RDN denote *a*ttractive-*d*ominant e*n*dothermic and *r*epulsive-*d*ominant e*n*dothermic respectively [25–28].

see Fig. 1, leaves the nature of the barrier with respect to rotation from the *trans* structure somewhat in doubt. Taking the 75°-*gauche* structure as typical of the *gauche* barrier gives a decomposition of $\Delta E_T$ indicative of a repulsive-dominant process, see Table 5 (iii). But, with the magnitude of $\Delta V_{nn}$ and $\Delta E_{elec}$ as small as this, it is quite possible that the use of a more extended basis set, or geometry optimization including electron correlation could lead to a reversal of signs.

### 3.4. *Total atomic charges*

A principal drawback of population analysis is its insensitivity to subtle polarization of the electron density, and, in addition, the results are often quite dependent on the basis set employed [29, 30]. So a preliminary survey was undertaken to establish how important this might be in the case of 1,3-butadiene by carrying out calculations on the *trans* structure using different basis sets, see Table 6. Qualitatively all but one of the charge distributions is found to be independent of the basis set employed.

The charge on the central C-atoms is little affected by the inclusion of polarization functions on the carbon, 6-31G → 6-31G*, although it does decrease a little at the 6-311G** level with the inclusion of polarization functions on the hydrogen. Although the charge on the terminal C-atoms is increased substantially by the inclusion of polarization functions on the carbon, it is then decreased even more by the inclusion of polarization functions on the hydrogen at the 6-311G** level. Nevertheless at all three levels the charge on the terminal C-atoms is greater than that on the central C-atoms.

Inclusion of polarization functions on the hydrogen at the 6-311G** level increases the charge on all three types of H-atom to a considerable extent. But, whereas the terminal side-chain H-atoms, $H_1$ and $H_{1'}$, still carry more charge than the chain H-atoms, $H_0$ and $H_{0'}$, there is a reversal with respect to the charge on the central side-chain H-atoms, $H_2$ and $H_{2'}$. At the 6-311G** level it is greatest on these H-atoms, but least at the 6-31G and 6-31G* levels.

Considered against the background of these results the changes in charge on $C_1$ and $C_{1'}$, $C_2$ and $C_{2'}$, $H_0$ and $H_{0'}$ and $H_1$ and $H_{1'}$, calculated using the 6-311G** basis set as the CCCC dihedral angle is varied from 180° through the region of

**Table 6.** Total atomic charges on the C- and H-atoms in *trans* 1.3-butadiene, calculated using different basis sets with full geometry optimization

| | | Basis Set | |
|---|---|---|---|
| Atom | 6-31G | 6-31G* | 6-311G** |
| $C_1, C_{1'}$ | 6.3754 | 6.4138 | 6.1787 |
| $C_2, C_{2'}$ | 6.1378 | 6.1398 | 6.1313 |
| $H_0, H_{0'}$ | 0.8330 | 0.8153 | 0.8887 |
| $H_1, H_{1'}$ | 0.8356 | 0.8201 | 0.8979 |
| $H_2, H_{2'}$ | 0.8182 | 0.8110 | 0.9034 |

**Table 7.** Total atomic charges on the C- and H-atoms in 1,3-butadiene as a function of the CCCC dihedral angle, calculated using the 6-311G** basis set

| Atom | 0° (*trans*) | 135° | 150° | 165° | 180° (*cis*) |
|---|---|---|---|---|---|
| $C_1, C_{1'}$ | 6.1787 | 6.1828 | 6.1784 | 6.1716 | 6.1684 |
| $C_2, C_{2'}$ | 6.1313 | 6.1362 | 6.1371 | 6.1406 | 6.1427 |
| $H_0, H_{0'}$ | 0.8887 | 0.8910 | 0.8888 | 0.8868 | 0.8860 |
| $H_1, H_{1'}$ | 0.8979 | 0.8954 | 0.8980 | 0.9006 | 0.9016 |
| $H_2, H_{2'}$ | 0.9034 | 0.8946 | 0.8977 | 0.9003 | 0.9013 |

the *gauche* minimum, are likely to be quite reliable, see Table 7. The charge on the terminal C-atoms increases, while the charge on the central C-atoms decreases. The charge on the chain H-atoms increases, while the charge on the side-chain terminal H-atoms decreases. The charge on the central side-chain H-atoms also decreases–to an even greater extent than the charge on the other H-atoms.

In passing from the *cis* structure to the more stable *gauche* minimum structure, the terminal C-atoms and the chain H-atoms thus tend to gain charge, whereas the central C-atoms and the other H-atoms tend to lose charge. Finally, on approaching the *trans* structure, all these changes with the exception of that on $C_2$ (and $C_{2'}$) are reversed.

## 4. Discussion

The calculations reported above strengthen the conclusion that the potential energy curve for rotation about the C—C bond in 1,3-butadiene is very flat in the region of the *cis* structure, and so the resulting *gauche* structures could well have comparable populations making the identification of the second stable conformer as any one unique structure difficult if not impossible experimentally [2, 3, 31]. The shape of the curve appears to be remarkably insensitive to the choice of geometry, the quality of the basis set employed, and the inclusion of electron correlation–very similar results being obtained in the present study as those utilizing the STO-3G basis set and limited geometry optimization involving only the CCC valence angle [8].

The finding that the *gauche* structures in the neighborhood of the *cis* structure are actually more compact, having more positive values of $V_{nn}$ contrary to expectation based on a rigid rotation model, shows their slightly greater stability relative to the *cis* structure to be due to a more favorable electronic energy, see Table 5, and not simply to a diminution in nuclear repulsion brought about by the torsion relieving the steric hindrance between the adjacent vinyl hydrogens, $H_1$ and $H_{1'}$. The *gauche* structures in the neighborhood of the *trans* structure on the other hand show just the opposite behavior, having less positive values of $V_{nn}$ relative to the *trans* structure, and are thus more relaxed.

To gain a more detailed understanding of the way these more compact and more relaxed *gauche* structures arise, $V_{nn}$ for the interconversion

*cis* structure → 150°-*gauche* structure

and

*trans* structure → 60°-*gauche* structure

has been split up into the individual contributions from the various nuclear-nuclear interaction terms.

Two types of internuclear distances can be distinguished – those which in a rigid rotation model would be dependent on the dihedral angle, and those which would not. With geometry optimization the latter undergo a small change, and the former have a small change superimposed on that due to the rotation. Bonded nuclei, in the chemical structure sense, are obviously rotation-independent, whereas nonbonded nuclei can be either, depending on the "bond" about which rotation occurs. In the rotation about the C—C bond in 1,3-butadiene sixteen of the internuclear distances are rotation-dependent and twenty-nine are rotation-independent, see columns 1 and 2 in Table 8.

In the case of the 150°-*gauche* structure the more positive $V_{nn}$ relative to the *cis* structure, +267 kJ mol$^{-1}$, is due mainly to the rotation-independent interactions $C_1 \cdots C_{2'}$ and $C_{1'} \cdots C_2$, accounting for +224 kJ mol$^{-1}$, with the other carbon–carbon interactions contributing a further +33 kJ mol$^{-1}$. The carbon–hydrogen interactions *in toto* also make a positive contribution, +45 kJ mol$^{-1}$; whereas the hydrogen–hydrogen interactions make a negative contribution, −35 kJ mol$^{-1}$, due principally to the rotation-dependent $H_1 \cdots H_{1'}$, the internuclear distance increasing from 2.34205 to 2.48065 Å thereby relieving the crowding in this region of the *cis* structure.

The conversion of the *trans* structure into the 60°-*gauche* structure presents a marked contrast. $\Delta V_{nn}$ is negative, −220 kJ mol$^{-1}$, and the individual contributions from the carbon–carbon interactions range in magnitude from about 90 to almost 600 kJ mol$^{-1}$. But the interplay of contributions of opposite sign results in a net contribution of only +29 kJ mol$^{-1}$. *In toto* the carbon–hydrogen interactions make the major contribution, 161 kJ mol$^{-1}$, with the hydrogen–hydrogen interactions contributing about half as much again, −89 kJ mol$^{-1}$. In this case it is to be noted that without exception rotation-dependent interactions make the largest contributions in each category, e.g. $C_1 \cdots C_{1'}$, $H_0 \cdots C_{1'}$, & $H_{0'} \cdots C_1$, $H_1 \cdots C_{1'}$ & $H_{1'} \cdots C_1$, $H_2 \cdots C_{1'}$ & $H_{2'} \cdots C_1$, and $H_1 \cdots H_{2'}$ & $H_{1'} \cdots H_2$.

The existence of more relaxed *gauche* structures in the region of the *trans* conformer is apparently not a feature unique to 1,3-butadiene. In their study of rotation about the C—C bond in glyoxal Sundberg and Cheung [32], using an even-tempered basis set, O(9,5)C(6,4)H(4), with partial geometry optimization for the *gauche* structures, found $V_{nn}$ for the 15°-*gauche* structure to be 168 kJ mol$^{-1}$ less positive than that for the *trans* conformer. Comparison of the

**Table 8.** Contributions to $\Delta V_{nn}$ for the conversion of (a) *cis* into 150°-*gauche* 1,3-butadiene, (b) *trans* into 60°-*gauche* 1,3-butadiene, and (c) *trans* into 90°-*gauche* 1.3-butadiene, from the changes in individual nuclear–nuclear interaction terms

| | | $\delta\Delta V_{nn}$ kJ mol$^{-1}$ | | |
|---|---|---|---|---|
| Nuclear interaction(s) | Type[a] | *Cis* → 150°-*gauche* | *Trans* → 60°-*gauche* | *Trans* → 90°-*gauche* |
| $C_1=C_2$ & $C_{1'}=C_{2'}$ | — | +33 | +188 | +229 |
| $C_1 \cdots C_{2'}$ & $C_{1'} \cdots C_2$ | — | +224 | −279 | −357 |
| $C_2-C_{2'}$ | — | +34 | −472 | −506 |
| $C_1 \cdots C_{1'}$ | R | −34 | +592 | +1286 |
| | | +257 | +29 | +652 |
| $H_0-C_1$ & $H_{0'}-C_{1'}$ | — | −5 | −9 | −12 |
| $H_0 \cdots C_2$ & $H_{0'} \cdots C_{2'}$ | — | −9 | +18 | +23 |
| $H_0 \cdots C_{2'}$ & $H_{0'} \cdots C_2$ | — | +10 | −24 | −29 |
| $H_0 \cdots C_{1'}$ & $H_{0'} \cdots C_1$ | R | +7 | +93 | −198 |
| $H_1-C_1$ & $H_{1'}-C_{1'}$ | — | −5 | −4 | +4 |
| $H_1 \cdots C_2$ & $H_{1'} \cdots C_{2'}$ | — | +23 | +5 | +12 |
| $H_1 \cdots C_{2'}$ & $H_{1'} \cdots C_2$ | — | +70 | −34 | −47 |
| $H_1 \cdots C_{1'}$ & $H_{1'} \cdots C_1$ | R | −59 | +305 | +694 |
| $H_2 \cdots C_1$ & $H_{2'} \cdots C_{1'}$ | — | −25 | +25 | +24 |
| $H_2-C_2$ & $H_{2'}-C_{2'}$ | — | −10 | −7 | −20 |
| $H_2 \cdots C_{2'}$ & $H_{2'} \cdots C_2$ | — | −18 | −75 | −69 |
| $H_2 \cdots C_{1'}$ & $H_{2'} \cdots C_1$ | R | +66 | −454 | −785 |
| | | +45 | −161 | −7 |
| $H_0 \cdots H_1$ & $H_{0'} \cdots H_{1'}$ | — | −3 | −1 | −2 |
| $H_0 \cdots H_2$ & $H_{0'} \cdots H_{2'}$ | — | −7 | +6 | +7 |
| $H_0 \cdots H_{2'}$ & $H_{0'} \cdots H_2$ | R | +3 | −29 | −51 |
| $H_0 \cdots H_{1'}$ & $H_{0'} \cdots H_1$ | R | +2 | +28 | +61 |
| $H_0 \cdots H_{0'}$ | R | +1 | +4 | +8 |
| $H_1 \cdots H_2$ & $H_{1'} \cdots H_{2'}$ | — | 0 | +1 | +1 |
| $H_1 \cdots H_{2'}$ & $H_{1'} \cdots H_2$ | R | +19 | −151 | −250 |
| $H_1 \cdots H_{1'}$ | R | −33 | +34 | +85 |
| $H_2 \cdots H_{2'}$ | R | −17 | +20 | +48 |
| | | −35 | −88 | −93 |
| $\Delta V_{nn}$ kJ mol$^{-1}$ | | +267 | −220 | +552 |

[a] "R" indicates that in a rigid rotation model the internuclear distance depends on the CCCC dihedral angle, i.e. is "rotation-dependent", whereas the other internuclear distances are invariant.

glyoxal and butadiene structures in relation to the $\delta\Delta V_{nn}$ in column 4 of Table 8 suggests that the rotation-dependent H···O interactions, corresponding to the $H_2 \cdots C_{1'}$ and $H_{2'} \cdots C_1$ interactions, are the dominant factor. However, since these interactions are just as important in rigid rotation where the relaxation of the *gauche* structures is not present, it would appear that the relaxation observed originates in the changes in geometry revealed by the optimization.

With dihedral angles greater than about 74°, $V_{nn}$ for the *gauche* structures of butadiene becomes more positive than that for the *trans* conformer and it is of interest to establish which interactions are primarily responsible for this reversal in behavior. The 90°-*gauche* structure, with a $\Delta V_{nn}$ of $+552$ kJ mol$^{-1}$ relative to the *trans*, has been chosen for this purpose because of its significance from the point of view of valence bond theory. In contrast to the planar *trans* and *cis* structures, in which $\pi$-electron delocalization is at a maximum, in the 90°-*gauche* structure the $\pi$-bond planes are perpendicular and delocalization is at a minimum, although hyperconjugation might exercise a small stabilizing effect [33].

Comparison of the $\delta\Delta V_{nn}$ values in columns 4 and 5 of Table 8 shows that not only are the rotation-dependent interactions which are predominant in the *trans*$\rightarrow$60°-*gauche* conversion also predominant in the *trans*$\rightarrow$90°-*gauche* conversion, but in addition they are all much greater, on average about twice as big. The result of this is that even though $\delta\Delta V_{nn}$ for $H_2\cdots C_{1'}$ & $H_{2'}\cdots C_1$ and $H_1\cdots H_{2'}$ & $H_{1'}\cdots H_2$ are $-785$ and $-250$ kJ mol$^{-1}$ respectively, these very substantial negative contributions are completely outweighed by $\delta\Delta V_{nn}$ for $H_0\cdots C_{1'}$ & $H_{0'}\cdots C_1$, $H_1\cdots C_{1'}$ & $H_{1'}\cdots C_1$ and $C_1\cdots C_{1'}$, $+198$, $+694$ and $+1286$ kJ mol$^{-1}$ respectively. The increase for $C_1\cdots C_{1'}$ is, in fact, so great that the net contribution from the carbon–carbon interactions is $+652$ kJ mol$^{-1}$ for the 90°-*gauche* conversion, compared to only $+29$ kJ mol$^{-1}$ for the 60°-*gauche* conversion. The net contribution from the carbon–hydrogen interactions is also, in effect, more positive, changing from $-161$ to $-7$ kJ mol$^{-1}$.

This kind of analysis brings out very clearly the importance of nonbonded interactions, not only in initiating the destabilization of the crowded *cis* structure, but also throughout the entire range of CCCC dihedral angles, 0° to 180°.

## 5. Appendix

### 5.1. Estimation of the correlation energy for trans-1,3-butadiene

The total molecular energy calculated from the expression E(molecule, fixed nuclei) $=$ E(atoms, fixed nuclei) $+ \Delta H_f^0$(0 K, molecule)

$$-\Delta H_f^\circ(0\ \mathrm{K,\ atoms}) - E_{\mathrm{vib}}(0\ \mathrm{K,\ molecule})$$

using energy values from the following references E(atoms, fixed nuclei) [34], $\Delta H_f^\circ$(298 K, molecule) [35], $H_{298}^\circ - H_0^\circ$(molecule) [36], $\Delta H_f^\circ$(0 K, atoms) [34] and $E_{\mathrm{vib}}$(0 K, molecule) [37], with the conversion factors 1 a.u. $\equiv$ 627.5095 kcal mol$^{-1}$ and 1 kcal $\equiv$ 4.184 kJ, is $-156.0393$ a.u..

The restricted Hartree–Fock limit molecular energy, $E_{RHF}$, estimated from the SCF energy of $-154.91905$ a.u. obtained using the 6-31G* basis set, Table 2, and an Ermler–Kern factor [38] of 1.000534(35) based on data for $C_1$ and $C_2$ hydrocarbons [39], is $-155.0018(54)$ a.u..

The correlation energy, defined as E(molecule, fixed nuclei) $-E_{RHF}$, is thus $-1.0375(54)$ a.u. From the molecular energies given in Table 2 it follows that about 51% of the correlation energy is accounted for at the MP3 level, and about 52% at the CI (size corrected) level. In the calculations of Dumbacher [9] and

Pincelli et al. [10] the inclusion of CI resulted in $E_T$ values more negative by 0.0365 and 0.2666 a.u. respectively, thereby accounting for about 4% and 26% of the correlation energy.

*Acknowledgement.* The authors gratefully acknowledge the generous grant of computer time provided by the computer center of the Philadelphia College of Textiles and Science.

## References

1. Carreira, L. A.: J. Chem Phys. **62**, 3851 (1975)
2. Squillacote, M. E., Sheridan, R. S., Chapman, O. L., Anet, F. A. L.: J. Am. Chem. Soc. **79**, 3657 (1979)
3. Mui, P. W., Grunwald, E.: private communication, 1981
4. Segre, A. L., Zetta, L., Corato, A. D.: J. Mol. Struct. **32**, 296 (1969)
5. Lipnick, R. L., Garbisch, E. W.: J. Am. Chem. Soc.: **95**, 6370 (1973)
6. Tyulin, V. I.: J. Struct. Chem. **15**, 639 (1974)
7. Bock, C. W., George, P., Trachtman, M., Zanger, M.: J. Chem. Soc., Perkin Trans II, 26 (1979)
8. Radom, L., Pople, J. A.: J. Am. Chem. Soc. **92**, 4786 (1970)
9. Dumbacher, B.: Theoret. Chim. Acta (Berl.) **23**, 346 (1972)
10. Pincelli, U., Cadioli, B., Levy, B.: Chem. Phys. Letters **13**, 249 (1972)
11. Skancke, P. N., Boggs, J. E.: J. Mol. Struct. **16**, 179 (1973)
12. Skaarup, S., Boggs, J. E., Skancke, P. N.: Tetrahedron **32**, 1179 (1976)
13. Cole, A. R. H., Mohay, G. M., Osborne, G. S.: Spectrochim. Acta, Part A **23**, 909 (1967)
14. Almenningen, A., Bastiansen, O., Traetteberg, M.: Acta Chem. Scand. **12**, 1221 (1958)
15. Kuchitsu, K., Fukuyama, T., Morino, Y.: J. Mol. Struct. **1**, 463 (1968)
16. Kuchitsu, K., Fukuyama, T., Morino, Y.: J. Mol. Struct. **4**, 41 (1969)
17. Haugen, W., Traetteberg, M. in Andersen, P., Bastiansen, O., Furberg, S. eds., Selected topics in structure chemistry p. 113. Oslo: Universitetsforlaget 1967; also Haugen, W., Traetteberg, M.: Acta Chem. Scand. **20**, 1726 (1966)
18. Aston, J. G., Szasz, G., Woolley, H. W., Brickwedde, F. G.: J. Chem. Phys. **14**, 67 (1946)
19. Roth, R.: private communication
20. Binkley, J. S., Whiteside, R. A., Krishnan, R., Seeger, R., DeFrees, D. J., Schlegel, H. B., Topiol, S., Kahn, L. R., Pople, J. A.: QCPE **13**, 406 (1981)
21. Hehre, W. J., Ditchfield, R., Pople, J. A.: J. Chem. Phys. **56**, 2257 (1972)
22. Hariharan, P. C., Pople, J. A.: Theoret. Chim. Acta (Berl.) **28**, 213 (1973)
23. Krishnan, R., Binkley, J. S., Seeger, R., Pople, J. A.: J. Chem. Phys. **72**, 650 (1980)
24. Pople, J. A., Seeger, R., Krishnan, R.: Int. J. Quant. Chem. Symp. **11**, 149 (1977)
25. Fink, W. H., Allen, L. C.: J. Chem. Phys. **46**, 2261 (1967)
26. Allen, L. C.: Chem. Phys. Letters **2**, 597 (1968)
27. Csizmadia, I. G., Theodorakopoulos, G., Schlegel, H. B., Whangbo, M.-H., Wolfe, S.: Canad. J. Chem. **55**, 986 (1977)
28. George, P., Bock, C. W., Trachtman, M., Brett, A. M.: Intern. J. Quantum Chem. **13**, 271 (1978)
29. Payne, P. W., Allen, L. C.: Barriers to rotation and inversion, in Applications of electronic structure theory, Schaefer III, H. F., ed. Chap. 2. New York: Plenum Press 1977
30. Fischer-Hjalmars, I., Siegbahn, P.: Theoret. Chim. Acta (Berl.) **31** 1 (1973)
31. Runge, W.: Structural Chemistry, in The Chemistry of ketenes, allenes and related compounds, Patai, S. ed. Chap. 2, p. 77. New York; John Wiley 1980
32. Sundberg, K. R., Cheung, L. M.: Chem. Phys. Letters **29**, 93 (1974)
33. Mulliken, R. S.: Tetrahedron **6** 68 (1959)
34. Pople, J. A., Binkley, J. S.: Mol. Phys. **29**, 599 (1975)
35. Pedley, J. B., Rylance, J.: Sussex-NPL. Computer Analysed Thermochemical Data: Organic and organometallic compounds. England: Univ. of Sussex 1977

36. Rossini, F. D., Pitzer, K. S., Arnett, R. L., Braun, R. M., Pimental, G. C.: Selected values of properties of hydrocarbons and related compounds. Pittsburgh; Carnegie Press 1953
37. Compton, D. A. C., George, W. O., Maddams, W. F.: J. Chem. Soc. Perkin II, 1666 (1976)
38. Ermler, W. C., Kern, C. W.: J. Chem. Phys. **61**, 3860 (1974)
39. George, P., Trachtman, M., Bock, C. W.: J. Comput. Chem. **2**, 334 (1981)

Received August 1, 1983